Exciton binding energy in T-shaped semiconductor quantum wires

S. N. Walck and T. L. Reinecke
Naval Research Laboratory, Washington, D.C. 20375

P. A. Knipp
Department of Physics and Computer Sciences, Christopher Newport University, Newport News, Virginia 23606

(Received 9 May 1997)

Exciton binding energies in semiconductor T-shaped quantum wires formed at the intersection of two quantum wells are given as functions of well width and potential offset. The calculations are made within the effective mass approximation using a variational approach for the exciton binding energy and numerical calculations for the nonseparable single particle electron and hole subband wave functions. Recent experimental results for these structures are discussed. [S0163-1829(97)04639-0]

The role of confinement in giving increased exciton binding energies through increased electron-hole overlap has been one of the most intensely studied aspects of the behavior of low-dimensional semiconductor systems in recent years. In most bulk III-V materials the exciton is not thermally stable at room temperature, but it becomes so with confinement, a property of considerable interest in a number of potential applications including modulators and switches. The increase of the exciton binding energy provides insight into the confinement of the electron and hole states, a key issue in understanding low-dimensional systems.

Exciton binding energies have been studied in detail experimentally in quantum wells, where values approaching the two-dimensional limit of four times the bulk binding energy have been observed. In an ideal one-dimensional system the exciton binding energy diverges,[1] and thus it is of interest to look to quantum wires for further enhancements of the binding energy. Recently experimental results have been reported for several wire structures including so-called V-groove wires,[2] serpentine superlattice quantum wire structures,[3] and wires formed by lithography and etching.[4] The binding energies in this interesting group of structures generally have been found to reach values in the range of $2\frac{1}{2}-3\frac{1}{2}$ times the bulk Rydberg.

T-shaped quantum wires (T wires) have been formed by the epitaxial overgrowth of cleaved edge GaAs/Al_xGa_{1-x}As quantum wells.[5] These structures exhibit high optical quality and are of interest in, for example, laser action. Work is being done aimed at determining sizes and structures to maximize the confinement energy.[6,7] The exciton binding energy is a significant part of the confinement energy in these structures, and thus it is an important part of a quantitative understanding of their properties. Recently an exciton binding energy of some six times the bulk value was reported in a GaAs/AlAs T-wire structure with 5.4 nm quantum wells.[8] Such a large value is somewhat surprising in light of the binding energies reported for other quantum wire structures.

It is worth noting that it is more difficult to obtain reliable experimental results for exciton binding energies in quantum wires than in bulk or quantum well systems. They cannot be extracted from magneto-optical data for quantum wires in the same straightforward way as in bulk or in quantum wells because the single particle energies have nonlinear magnetic field dependences.[9] In order to obtain them directly from luminescence data, the single particle energies must be known accurately. Often the binding energies are estimated from exciton diamagnetic shifts[2,4] using models, with the introduction of possible uncertainties.

Recently we have shown that detailed variational calculations of exciton binding energies are in good agreement with experimental results for modulated-barrier and deep-etched wires and dots of widely varying sizes formed by lithography and etching.[4] In the present paper we give corresponding results for semiconductor T-wire structures. The calculations are made using numerical results for the nonseparable single particle electron and hole states. Results for the binding energies are given here as functions of well width and of potential offset.

A sketch of the T-wire structure is shown in Fig. 1. Here $\hat{\mathbf{x}}$ is along the direction of the first growth (that of QW1), $\hat{\mathbf{y}}$ in that of the second growth (of QW2), and $\hat{\mathbf{z}}$ in the direction of the quantum wire. We take the effective mass Hamiltonian for an exciton in a T-wire structure to be

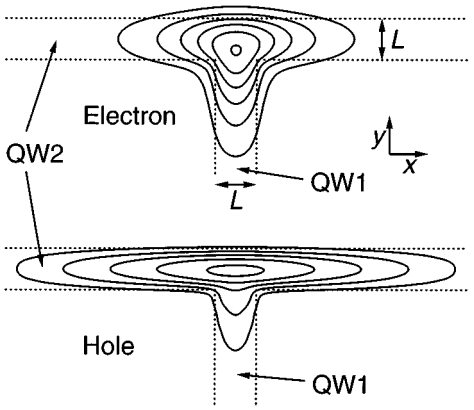

FIG. 1. Cross-sectional diagram of the T-wire structure. Quantum well widths are L. Also shown are contour plots of single particle electron and hole wave functions for $L = 5.4$ nm and $Al_{0.3}Ga_{0.7}As$ barriers.

TABLE I. Material parameters.

	QW1	QW2	Barrier
m_e	0.0665	0.0665	$0.0665+0.083x$
m_{hx}	0.38	0.15	0.38
m_{hy}	0.15	0.71	0.38
m_{hz}	0.15	0.15	0.38
ϵ	12.5	12.5	12.5

$$H=\frac{p_{x_e}^2+p_{y_e}^2+p_{z_e}^2}{2m_e}+\frac{p_{x_h}^2}{2m_{hx}}+\frac{p_{y_h}^2}{2m_{hy}}+\frac{p_{z_h}^2}{2m_{hz}}+V_e(x_e,y_e)+V_h(x_h,y_h)-\frac{e^2}{\epsilon|\mathbf{r}_e-\mathbf{r}_h|}. \quad (1)$$

We take the conduction band to be isotropic with a single effective mass for the electron in each material.[10] In general, in these materials the valence band is composed of light and heavy hole bands described by a Luttinger Hamiltonian. In the quantum wells these bands are split, and we represent the valence band in each well by an anisotropic parabolic band with one mass parallel to the well and another perpendicular to it and with the hole masses chosen from the diagonal terms of the appropriate Luttinger Hamiltonian. In the barriers the holes are represented by a single isotropic effective mass.

The material parameters used here are given in Table I. They are appropriate for a structure with $\hat{\mathbf{x}}$ along the [001] direction, $\hat{\mathbf{y}}$ along the [110] direction, and $\hat{\mathbf{z}}$ along the $[1\bar{1}0]$ direction, which is the geometry studied in recent experiments.[5,8] $V_e(x_e,y_e)$ and $V_h(x_h,y_h)$ are the confining potentials for the electron and the hole, which are determined by the conduction and valence band offsets.[11] We take the fractions of the offsets in the conduction and valence bands to be 65% and 35% of the total offset. The dielectric constant ϵ is taken to be 12.5.[12]

A two-parameter nonseparable variational function[13] is used for the exciton,

$$\Psi(\mathbf{r}_e,\mathbf{r}_h)=\phi_e(x_e,y_e)\phi_h(x_h,y_h)\times e^{-\sqrt{\alpha^2[(x_e-x_h)^2+(y_e-y_h)^2]+\beta^2(z_e-z_h)^2}} \quad (2)$$

in which α and β are the variational parameters. The single particle wave functions $\phi_e(x_e,y_e)$ and $\phi_h(x_h,y_h)$ are the ground states of the single particle Hamiltonians for motion in the xy plane,

$$\left[\frac{p_{x_e}^2+p_{y_e}^2}{2m_e}+V_e(x_e,y_e)\right]\phi_e(x_e,y_e)=E_e\phi_e(x_e,y_e),$$

$$\left[\frac{p_{x_h}^2}{2m_{hx}}+\frac{p_{y_h}^2}{2m_{hy}}+V_h(x_h,y_h)\right]\phi_h(x_h,y_h)=E_h\phi_h(x_h,y_h). \quad (3)$$

The exciton binding energy is found in the usual way by minimizing

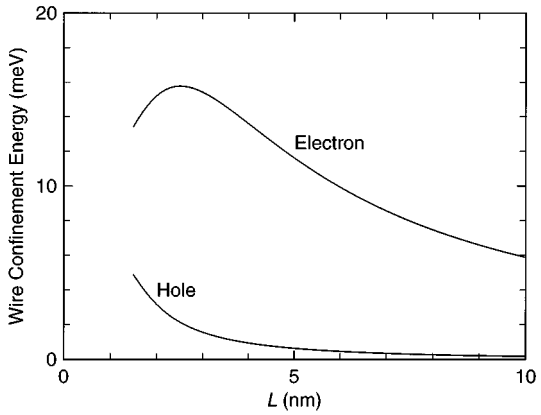

FIG. 2. Wire confinement energies for the electron and the hole as a function of T-wire well width, L. Results shown are for the case of $Al_{0.3}Ga_{0.7}As$ barriers.

$$E=\min_{\alpha,\beta}\frac{\langle\Psi|H|\Psi\rangle}{\langle\Psi|\Psi\rangle}, \quad (4)$$

and is given by $E_B=E_e+E_h-E$, where E_e and E_h are the single particle electron and hole energies.

The single particle wave functions in this geometry are nonseparable. The energies and wave functions are computed here by diagonalizing each single particle Hamiltonian in a basis of two-dimensional harmonic oscillator eigenstates. This method is desirable because the harmonic oscillator states are a complete, localized set of states and analytic expressions can be obtained for the matrix elements. A set of 900 basis functions was used in the diagonalization.

Electron and hole wave functions for 5.4 nm wires with $Al_{0.3}Ga_{0.7}As$ barriers are shown in Fig. 1, and the corresponding electron and hole confinement energies are shown in Fig. 2 as functions of size. The hole wave function is preferentially located in QW2 because the mass perpendicular to the well is larger in it than is the perpendicular mass in QW1. The localization energy of the hole is small, considerably less than that for the electron. Nevertheless, the confined hole wave function must be represented well in order to describe the electron-hole overlap properly. The confinement energies of the electron and hole are generally in agreement with earlier calculations.[6,14]

The exciton energy is evaluated for each α and β using the results of the single particle wave functions in the exciton function in Eq. (2). Five dimensional integrals are needed for each α and β. The integrals are carried out numerically using an adaptive algorithm.[15] Figure 3 shows the calculated exciton binding energies as functions of the quantum well width for $Al_{0.3}Ga_{0.7}As$ and AlAs barriers. The widths of the two quantum wells in the structure have been taken to be equal. The binding energies increase with decreasing structure size until a width of 1–2 nm is reached. For wires smaller than 1–2 nm the binding energy decreases for both types of barriers, indicating that a significant part of the exciton wave function is extending into the barrier region.

The effects of confinement on the single particle states and on the excitons can be modified by changing the potential barriers. Physically this can be achieved by varying the Al concentration in the barrier regions. Figure 4 gives the

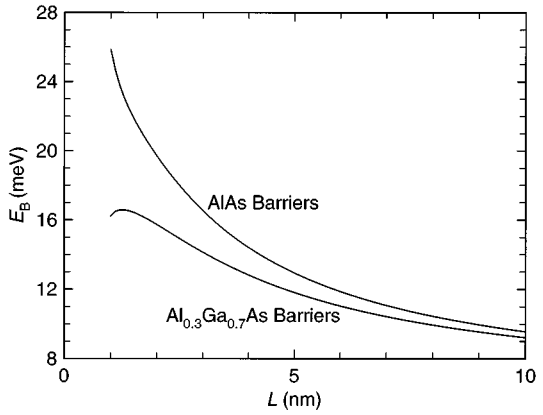

FIG. 3. Exciton binding energy E_B as a function of T-wire well width L for $Al_{0.3}Ga_{0.7}As$ and AlAs barriers.

effects of variations in the potential on the exciton binding energy for T wires with quantum wells of (equal) 5.4 nm widths. It is seen that the binding energy has only a modest dependence on the potential offset. This relatively weak dependence is consistent with the weak dependence on potential height seen in lithographically formed structures.[4] The Al concentration corresponding to the varying potential offset is also shown in Fig. 4.[11]

The hole masses in these systems are larger than the electron mass, and therefore we expect that the exciton binding energy should not be especially sensitive to details of the representation of the valence band. On the other hand, it is important to represent the electron-hole overlap well in the exciton, and we can see from Fig. 1 that the hole wave function depends on the anisotropic hole mass. As a measure of this effect, the exciton binding energy calculated for 5.4 nm wells with $Al_{0.3}Ga_{0.7}As$ barriers using a single isotropic hole mass of 0.38 everywhere is 15.2 meV as compared to 11.5 meV calculated here. For an isotropic hole mass, the asymmetry in the hole wave function seen in Fig. 1 is not present, and as a result the electron-hole overlap is larger.

The exciton binding energies have been checked as functions of the number of basis functions in the single particle

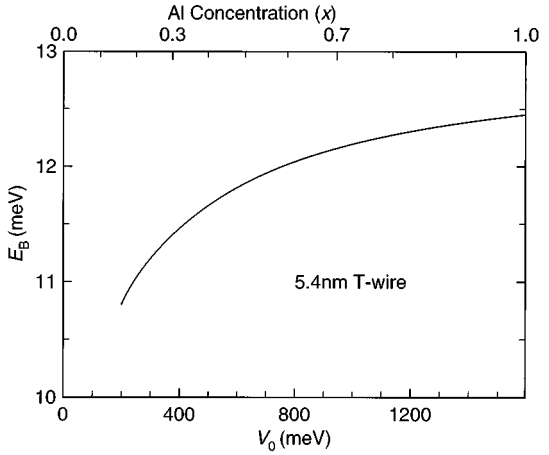

FIG. 4. Exciton binding energy E_B as a function of Al concentration x and of confinement potential V_0 for a 5.4 nm T wire. The upper horizontal scale is the Al concentration and the lower scale is the total (electron + hole) band offset in meV.

calculations, and we find that they are satisfactorily converged. The single particle energies and wave functions have also been calculated using the boundary element method[16] which we have developed recently for such problems, and they are in good agreement with those obtained from the calculations here. We have compared the present variational calculations based on Eq. (2) with the results of detailed numerical calculations for excitons in quantum wells done by expanding the exciton wave function in a basis of products of hydrogenlike states with electron and hole overlap functions, and we find that they agree well. We have also compared these variational results with simpler variational forms. For a single parameter variational wave function given by $\alpha=\beta$ in Eq. (2) the binding energy for 5.3 nm wells and AlAs barriers is 12.2 meV as compared to 12.5 meV obtained here. With a simpler two parameter separable form used in Ref. 7, we obtain 10.5 meV for the binding energy. Thus we see that the binding energy increases with increasing flexibility in the variational wave function.

From the present calculations we see that exciton binding energies in semiconductor T-wire structures are enhanced considerably over those in the bulk and also over the corresponding quantum well case. For $Al_{0.3}Ga_{0.7}As$ barriers the binding energy reaches over 3 times the bulk value of 4.9 meV for wire widths of 1–2 nm, and for AlAs barriers it reaches over 5 times the bulk value for wire widths near 1 nm. The binding energies have a significant dependence on the size which indicates that this effect must be included in considering the size dependence of the localization energy in the T-wire structures.

From recent photoluminescence studies, Someya *et al.*[8] reported exciton binding energies of $\sim$ 17 meV for a 5.4 nm T wire with $Al_{0.3}Ga_{0.7}As$ barriers and $\sim$ 27 meV for a 5.3 nm T wire with AlAs barriers. These values are considerably greater than our results of 11.5 meV and 12.5 meV, respectively, for these two structures. In their experiments, they measured the difference between the position of the exciton lines in photoluminescence for the quantum wire and for the quantum well and evaluated the wire binding energy by using estimates of the single particle confinement energies based on model calculations and used an experimental value for the exciton binding energy for the well. There are uncertainties in all of the quantities. In particular, the single particle confinement energies vary by several meV for modest variations in the band structure parameters. In addition, recent experimental values for exciton binding energies in wells are lower.[17] We feel that the uncertainties in these values led to the large estimate of the binding energy in the analysis in Ref. 8.

Recently, calculations were reported using a method based on semiconductor Bloch equations[18] which gave exciton binding energies of 11.63 meV and 13.90 meV for the $GaAs/Al_{0.3}Ga_{0.7}As$ and GaAs/AlAs systems.[19] Their values are generally in accord with the present results.

We are grateful to E. Molinari and F. Rossi for communicating the results of their work to us. This work was supported in part by the U.S. Office of Naval Research. T.L.R. gratefully acknowledges the support of the Alexander von Humboldt Foundation during part of this work.

[1] R. Louden, Am. J. Phys. **27**, 649 (1959); R. J. Elliott and R. Louden, J. Phys. Chem. **8**, 382 (1959).
[2] R. Rinaldi, R. Cingolani, M. Lepore, M. Ferrara, I. M. Catalano, F. Rossi, L. Rota, E. Molinari, P. Lugli, U. Marti, D. Martin, F. Morier-Gemoud, P. Ruterana, and F. K. Reinhart, Phys. Rev. Lett. **73**, 2899 (1994).
[3] H. Weman, M. Potemski, M. E. Lazzouni, M. S. Miller, and J. L. Merz, Phys. Rev. B **53**, 6959 (1996).
[4] M. Bayer, S. N. Walck, T. L. Reinecke, and A. Forchel, Europhys. Lett. (to be published).
[5] A. R. Goñi, L. N. Pfeiffer, K. W. West, A. Pinczuk, H. U. Baranger, and H. L. Stormer, Appl. Phys. Lett. **61**, 1956 (1992).
[6] W. Langbein, H. Gislason, and J. M. Hvam, Phys. Rev. B **54**, 14 595 (1996).
[7] A. A. Kiselev and U. Rössler, Semicond. Sci. Technol. **11**, 203 (1996).
[8] T. Someya, H. Akiyama, and H. Sakaki, Phys. Rev. Lett. **76**, 2965 (1996).
[9] See, for example, M. Bayer, A. Forchel, I. E. Itskevich, T. L. Reinecke, P. A. Knipp, Ch. Gréus, R. Spiegel, and F. Faller, Phys. Rev. B **49**, 14 782 (1994).
[10] In treating cases in which the Al concentration of the barriers increases up to pure AlAs, we neglect any effects from the crossing of the Γ and X points of the conduction bands and take the electrons to be described by an isotropic effective mass which varies linearly with Al concentration.
[11] Total (electron + hole) potential offset is given in meV as a function of Al concentration x by $\Delta E_g(x)=1247x$ for $0\leqslant x\leqslant 0.45$ and $\Delta E_g(x)=1247x+1147(x-0.45)^2$ for $0.45<x\leqslant 1$. See, for example, H. C. Casey and M. B. Panish, *Heterostructure Lasers* (Academic Press, New York, 1978), Part A.
[12] The small effects of image charges due to the differences of the dielectric functions of the two materials are neglected here.
[13] Y. Shinozuka and M. Matsuura, Phys. Rev. B **28**, 4878 (1983); **29**, 3717 (1984).
[14] W. Wegscheider, L. N. Pfeiffer, A. Pinczuk, K. W. West, M. M. Dignam, R. Hull, and R. E. Leibenguth, J. Cryst. Growth **150**, 285 (1995).
[15] J. Berntsen, T. O. Espelid, and A. Genz, ACM Trans. Math. Softw. **17**, 437 (1991).
[16] P. A. Knipp and T. L. Reinecke, Phys. Rev. B **54**, 1880 (1996).
[17] M. Gurioli, J. Martinez-Pastor, M. Colocci, A. Bosacchi, S. Franchi, and L. C. Andreani, Phys. Rev. B **47**, 15 755 (1993).
[18] F. Rossi, G. Goldoni, and E. Molinari, Phys. Rev. Lett. **78**, 3527 (1997).
[19] These authors earlier reported higher values of the exciton binding energies (Ref. 20) in agreement with the experimental results of Ref. 8 based on such calculations.
[20] F. Rossi and E. Molinari, *23rd International Conference on the Physics of Semiconductors*, edited by M. Scheffler and R. Zimmermann (World Scientific, Singapore, 1996), p. 1161.